ISSN 2278-2540 | DOI: 10.51583/IJLTEMAS | Volume XV, Issue VIII, August 2026

Joule Heating Effects on Isotachophoretic Preconcentration of Analytes

Priyanka Kumari[1] , Ujjwal Kanti Ghoshal[2*]

[1]Department of Mathematics, Veer Kunwar Singh University Ara, Ara-802301, India

[2]Department of Mathematics, S. P. Jain College, Veer Kunwar Singh University Ara, Ara-802301, India

***Corresponding Author**

DOI: https://doi.org/10.51583/IJLTEMAS.2026.150800066

Received: 28August 2026; Accepted: 02 September 2026; Published: 12 September 2026

ABSTRACT

We investigate the effect of Joule heating on the pseudosteady-state behaviour of the isotachophoretic transport of ionic species in a 2-D microchannel with both ends kept at constant temperature. The Joule heating-induced temperature gradient may significantly alter ion transport by changing the thermophysical properties. The equations governing the phenomena are the Nernst-Planck equations for transport of ions coupled with the equation for temperature field. A finite volume based QUICK (Quadratic Upwind Interpolation Convection Kinematics) scheme is used to compute the governing equations. The stack of ionic species in the channel occurs according to the increasing order of electrical conductivity or decreasing order of electric field. The heat generation is highest at the region filled by low conducting electrolyte (TE) and leads to a high temperature plateau. An inclination in temperature profile arises across the transition zones between two consecutive stacks of analytes. Our result shows that the ITP velocity for temperature dependent case no longer varies linearly with the applied electric field. The migration speed is greatly influenced by the ionic concentration of the sample. A parametric study is made to investigate the minimal Joule heating effect on ITP transport of analytes.

Keywords: Joule heating effect, Energy equation, QUICK scheme, Transient state, Sample zone.

INTRODUCTION

Isotachophoresis (ITP) is an electromigration separation technique based on the difference in migration speed of the electrolytes under influence of external electric field. The name derives from the fact that, in the final stage of the separation process, zones of the individual electrolytes are formed moving with the same speed and ordered according to the ion migration speeds. ITP is carried out between two homogeneous solutions: a leading electrolyte (LE) of higher electrophoretic mobility and a terminating electrolyte (TE) of lower electrophoretic mobility. Upon application of an electric field, a sharp transition zone is formed between the two buffers which migrate towards the part of the channel occupied by the LE at a uniform speed. The small width of an ITP transition zone and the large difference in properties between the LE and TE regions lead to large gradients in electric field and concentrations. Thus, ITP separation is accomplished by a self-sharpening effect due to stepwise change in conductivity across the transition zone. It is a widely used technique which can isolate charged biological particles such as proteins, DNA and RNA. The principles and applications of ITP have already been fully described by several earlier reviews ([1]- [2]).

Several numerical methods have been proposed in resolving the interface zones in ITP ([3]- [9]). Most of the previous works are based on the one-dimensional computation of ITP. Joule heating effect is unavoidable in electrophoretic transport phenomena where ionic species migrate due to an applied voltage drop. A numerous studies have been conducted to investigate the effects of Joule heating on ions transport (Xuan and Li [10], Kates and Ren [11], Grushka et al. [12]). This effect, especially significant when high voltage drop is applied and it produces temperature gradient across the channel (Kang et al. [13] and the references there in). The Joule heating

ISSN 2278-2540 | DOI: 10.51583/IJLTEMAS | Volume XV, Issue VIII, August 2026

induced temperature gradient leads significant changes in electrophoretic transport of ions by changing the thermophysical properties. Due to the internal heat source, the microfludic device may overheat and it requires coolant surrounding the capillary by special equipment or by the cold liquid inside reservoirs. Therefore, it remains important to control the liquid temperature in microfluidic systems. On the contrary temperature induced effect is advantageous for speeding up the capillary electrophoresis separation process (see Rogacs and Santiago [14]). It may be noted that the peak broadening and separation efficiency significantly influenced by Joule heating effect (Knox [15], Xuan and Li [10]). So far most of the studies are based on weak electric field assumption to minimize the Joule heating effect. Recently Shim and Dutta [21] studies the Joule heating effect on concentration boundaries in ITP and found a profound effect of temperature field on the ITP transport phenomena. The significant Joule heating effect makes a gradual difference in the band location across the channel. Thermal end effect on the electrosmotic transport of homogenous buffer are studied extensively by Xuan et al. [22]. In ITP which involves discontinuous electrolytes that suffers a nonuniform temperature field across the channel. However, to date, little has been reported on Joule heating effect in discontinuous buffer system having with distinct mobility. In this article, we present a computational study of Joule heating effect on the ITP by using finite volume based second order upwind scheme QUICK to resolve efficiently the sharpness which arise in the ITP transport. The thermophysical properties are considered to be dependent on temperature and hence the concentration distribution, electric field and temperature distribution across the channel are coupled. We present a quantative measurement of influence of heating effect on the migration speed of the ions. We have analyzed the dependence of the Joule heating effect on the sample distribution for several values of parameters governing the problem.

Mathematical Model & Numerical Methods

this article the isotachophoretic transport of ionic species in a straight 2-D channel with rectangular cross-section of length L and height H is considered. Both end of the channel are kept at a fixed temperature T_∞. Initially, the temperature across the flow domain considered to be uniform and kept at room temperature $T_\infty = 298\text{K}$. Throughout our study we have considered the ideal situation i.e., under no bulk fluid flow. The thermophysical properties like thermal conductivity $\boldsymbol{k}$, diffusion coefficients D_i of the electrolytes are considered to be temperature dependent. Due to the coupling nature of the thermophysical properties with temperature, the electric potential field, concentration of the ionic species present in the system and temperature field are strongly coupled. We consider a cationic ITP due to monovalent ions and denote the electrolyte of higher mobility by LE and lower one by TE. Let the concentration of LE and TE be C_l and C_t , respectively, concentration of sample species is C_s and the concentration of the common anion be C_0. The equation for ion transport is governed by Nernst-Planck equation,

$$\frac{\partial C_i}{\partial t} + \nabla \cdot [(\boldsymbol{q} + z_i \mu_i(T)\boldsymbol{E})C_i] - \nabla \cdot [\nabla D_i(T) C_i] = 0 \qquad (1)$$

Here $D_i(T)$, $\mu_i(T)$, z_i denotes, respectively the diffusion coefficient, electrophoretic mobility and valency of the i-th ionic species, where $i = l, t, s \; or \; 0$ denotes respectively, the TE cation, LE cation, sample species or common anion. Considering monovalent species, we set $z_i = 1 \; (i = l, t, s) and \; z_0 = -1$. The temperature dependent diffusivity of the ith ionic species is given by (Shim and Dutta [21]; Tang and Yang [23])

$$D_i(T) = D_{i,ref}[1 + 0.02(T - T_\infty)]$$

Where $D_{i,ref}$ is the diffusion coefficient at an ambient temperature $T_\infty = 298K$. The electrophoretic mobility and diffusivity at room temperature are related via Nernst-Einstein relation $\mu_i = D_i F/RT$, where F is Faraday constant, R is gas constant and T is absolute temperature.

ISSN 2278-2540 | DOI: 10.51583/IJLTEMAS | Volume XV, Issue VIII, August 2026

The net charge density ρ_e is defined as $\rho_e = F\sum_i z_i C_i$. When bulk concentration of the electrolyte is higher than $10^{-4}M$ the Debye length is of the order of few nano-meters. The length scale is far grater than the Debye length permits to invoke the electrical neutrality condition. Electroneutrality assumption allows us to eliminate the equation for C_0, which is obtained as $C_0 = C_t + C_s + C_l$. Through out this study we have consider the ideal situation i.e., $\boldsymbol{q} = 0$.

The electric field $E = -\nabla\phi$ is governed by well known Charge conservation principle and is given by

$$\nabla \cdot [\sigma(T)E] = \nabla.[F\sum_i D_i(T) z_i \nabla C_i] \qquad (2)$$

Where electrical conductivity $\sigma(T) = F\sum_i \mu_i(T) z_i^2 C_i$. The Joule heating temperature is governed by transport equation

$$\rho C_p \left[\frac{\partial T}{\partial t} + (q \cdot \nabla)T\right] = \nabla \cdot [k(T)\nabla T] + \sigma(T)(E.E) \qquad (3)$$

Where σ and C_p is the density and specific heat capacity of the liquid. The first and second term of right hand side represents respectively the thermal energy generation due to thermal diffusion

and Joule heating effect. The temperature dependent thermal conductivity *k(T)* is assumed to be (Shim and Dutta [21]; Tang and Yang [23])

$$k(T) = k_{ref}[1 + 0.0012(T - T_\infty)],$$

The height H of the channel is taken to be the length scale; concentration, potential and time are scale by C_l^∞, the bulk concentration of LE, $\phi_0 = RT/F$ and $\tau = \rho C_p H^2/k_{ref}$, respectively. The dimensionless temperature is defined by $\Theta = (T - T_\infty)/\Theta_{ref}$, where $\Theta_{ref} = \phi_0^2 \sigma_{ref}/k_{ref}$ with $\sigma_{ref} = F^2 C_l^\infty D_{l,\infty}/RT$ is the reference conductivity at ambient temperature. The non-dimensional equations for temperature filed, concentration of ionic species and potential field are

$$\frac{\partial \Theta}{\partial t} = \nabla.[f(\Theta)\nabla\Theta] + \sigma(\Theta)|\nabla\phi|^2 \qquad (4)$$

$$\frac{\partial c_i}{\partial t} - z_i Pe_i \nabla.[g(\Theta)c_i\nabla\phi] - Pe_i\nabla.[\nabla g(\Theta)c_i] = 0 \qquad (5)$$

$$-\nabla.[\sigma(\Theta)\nabla\phi] = \nabla.\left[\sum_i \frac{D_{i,\infty}}{D_{l,\infty}} g(\Theta) z_i \nabla c_i\right] \qquad (6)$$

where c_i is non-dimensionless concentration and scaled electrical conductivity is defined as

$$\sigma(\Theta) = \left[\sum_i \frac{D_{i,\infty}}{D_{l,\infty}} g(\Theta) c_i\right]$$

The functions $f(\Theta)$ and $g(\Theta)$ are defined as

$f(\Theta) = 1 + 0.02\Theta_{ref}\Theta$ and $f(\Theta) = 1 + 0.0012\Theta_{ref}\Theta$. At $T_\infty = 298K$, the reference thermal conductivity is $k_{ref} = 0.61 w/mK$ (Shim and Dutta [21]; Tang and Yang [23]). It may

ISSN 2278-2540 | DOI: 10.51583/IJLTEMAS | Volume XV, Issue VIII, August 2026

be noted that for isothermal case the correction term in $f\ (\Theta)$ and $g(\Theta)$ set to be zero and their values will be 1. The net flux through the channel walls are set to be zero, i.e.,$N_i\hat{n} = 0$ for $i = t, s\ or\ l,$ where $\hat{n}$ is the unit outward normal. The electric potential is subjected to insulating boundary conditions along the wall. We imposed symmetry boundary conditions for c_i (i.e., axial gradient of c_i is zero) across both the end of the channel. To study the Joule heating induced effect on the concentration boundaries, we consider $T = T_\infty$ i.e., $\Theta = 0$ along the inlet and outlet of the channel. The adiabatic boundary condition is considered along the channel wall. To start the ITP process, a voltage drop E_0L is applied across the channel, where E0 is the imposed electric field strength.

We have computed the equations for ion transport, electric field and heat transfer equation in a coupled manner through the finite volume method ([24]). We adopted the upwind scheme QUICK (Quardratic Upwind Interpolation Convection Kinematics) due to Leonard [25] to discretize the electromigration and convection terms in the ion transport equations. The diffusion fluxes at the control volume interfaces are estimated by linear interpolation between two neighbors to the either side of the control volume interfaces. The time derivatives are discretized through a first order implicit scheme. A detailed discussion onthis algorithm is presented elsewhere (Bhattacharyya and Gopmandal [19]; Bhattacharyya et al. [20]).

At any time level, we use an iterative procedure for the computation of ion transport equations as these equations are coupled with the charge conservation equation and temperature field. The iteration procedure starts with an assumption for potential at each cell and temperature field. Initially the temperature at each point of the computational domain is taken to be the ambient temperature. At every iteration, the electric field is determined by solving the charge conservation equation. After solving the concentration equations and charge conservation equation, we have solved the energy equation for temperature field.

RESULTS AND DISCUSSIONS

To illustrate the influence of thermal effect on ITP transport we considered five ionic components as given in Table-1. We compare our computed solution for temperature independent electrophoretic mobility case (constant μ_i) with the analytical expression of the concentration LE and TE as well as the axial electric field as given in Goet et al. [26]. Our computed results (Fig. 1a and b) is agrees well with the analytical solution. For the presence of different electrolyte in different portion of the channel a sharp change in electrolyte conductivity appear near the transition zone. The width of such zone under no bulk fluid flow is given by $\Delta X = 4\phi_0/\Delta E$, where ΔE is the difference in electric field strength at both the ends.

For a channel filled symmetrically by high conducting LE and low conducting TE, change in electric field strength ΔE can be written as $\Delta E = 2\phi_0(1 + D_r)/E_0(1 - D_r)$, where D_r is the ratio of electrophoretic mobility of TE with LE and E0 is applied electric field strength. The change in electrophoretic mobility due to Joule heating effect are in same order, so electrophoretic mobility ratio remains unaltered. So for constant electric filed strength, the transition zone.

Table 1. Valance and absolute electrophoretic mobility of different ionic components

Components	Valance	$D_{i,ref}$
Cl^-(counterion)	-1	$2.04 \times 10^{-9} m^2/s$
K^+(LE)	1	$1.94 \times 10^{-9} m^2/s$
Na^+(Sample-1)	1	$1.44 \times 10^{-9} m^2/s$
$C_4H_9N^+$(TE)	1	$2.04 \times 10^{-10} m^2/s$

ISSN 2278-2540 | DOI: 10.51583/IJLTEMAS | Volume XV, Issue VIII, August 2026

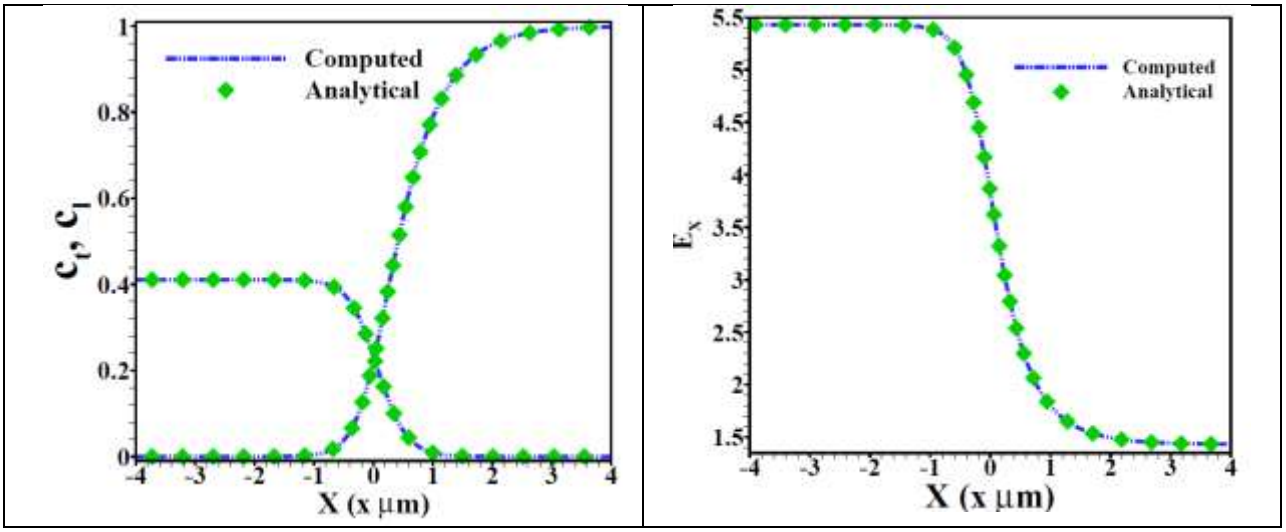

Figure 1. Comparison of concentration distribution of LE and TE and axial electric field E_x for ideal ITP case with the analytical results due to Goet et al. [26]. Here electric field is taken to be $E = 10^{-3}M$.

Due to the temperature dependence of the thermophysical properties, the correction term for the electrophoretic mobility of each ionic species and the thermal conductivity are linear functions of the temperature increment. This can lead to a gradual difference between thermally dependent and independent cases. The volumetric heat generation in the system due to the Joule heating effect is given by$(\sigma_{ref}\phi_0^2/H^2)\ \sigma(\Theta)(\mathbf{E}.\mathbf{E})$. It depends explicitly on the electric field strength, the ionic concentration of the electrolyte, and the electrophoretic mobility of the ionic species. To study the thermal effects on ITP separation, one need to consider the effect of all those key parameters. Unless stated otherwise, we consider the channel height $H = 1mm$.

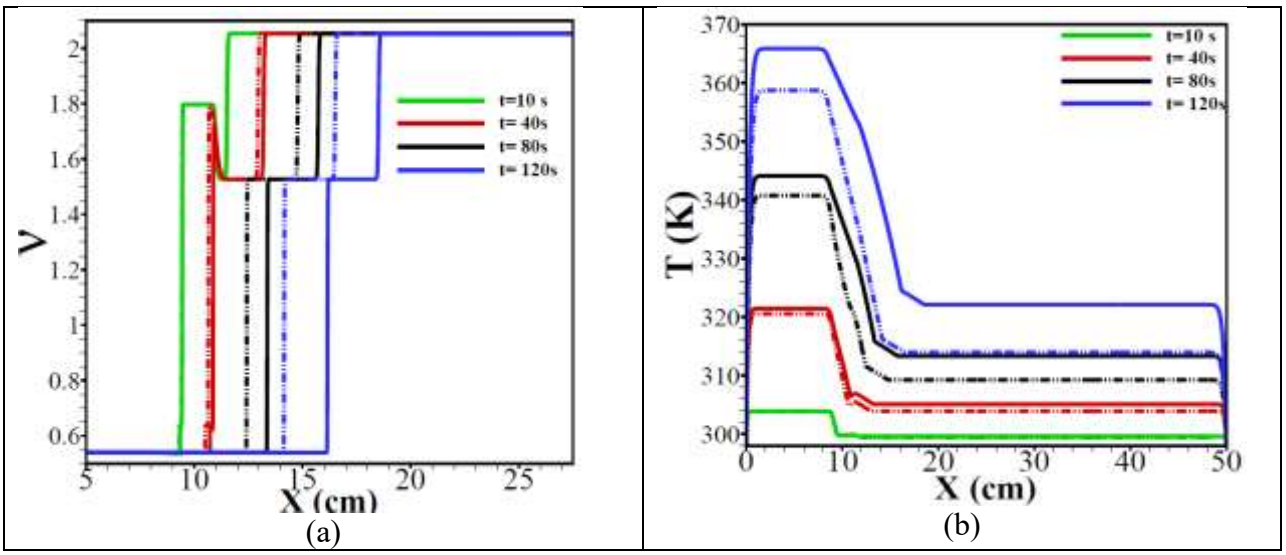

Figure 2. (a) Electrical conductivity and (b) axial temperature profile for fixed amount of sample species (Sample-1) presents in the system $M_s = 20mm \times HC_l^{\infty}$ at different time level. Here electric field applied $E_0 = 10^4 V/m$ and the concentration of the LE taken $C_l^{\infty} = 10^{-3}M$. The solid line represent the case when the electrical conductivity is depends on temperature and dotted line for temperature independent conductivity.

The transient behavior ITP is shown in Fig. 2 for temperature/ independent electrophoretic diffusivity of the electrolytes. The electric field $E_0 = 10^4 V/m$ is applied across the channel. The initial molar mass of the sample species considered to be $M_s = 20mm \times HC_l^{\infty}$ with $C_l^{\infty} = 10^{-3}M$. At the early stage of ITP separation, the concentration profiles does not much effected by the temperature induced Joule heating effect and the ionic

ISSN 2278-2540 | DOI: 10.51583/IJLTEMAS | Volume XV, Issue VIII, August 2026

species moves towards the ends of opposite polarity with almost same velocity. This is due to the fact that the diffusivity of the ionic species doesn't much influenced by the Joule heating effect at the early stage. As time goes on, the electrophoretic velocity of the ionic species is elevated due to Joule heating effect. We have shown the variation of electrical conductivity across the channel in Fig. 2(a). The zone filled with TE is low conducting and it leads a higher electric field near the inlet reservoir. The ionic species stacks along the channel according to electrical conductivity in increasing order and results the electric field in decreasing order.

To support this statement we have shown the transient behavior of temperature profile in Fig. 2(b). The volumetric heat generation in the system are due to Joule heating effect and thermal diffusion. From Fig. 2(b), it is clear that for fixed thermal conductivity of the electrolyte, the heat generation in the system is higher for the thermal dependent electrical conductivity.

The magnitude of the source term in the energy conservation equation increases when temperature dependence on electrical conductivity is taken into account and it leads an increment in heat generation into the system. A sharp temperature drop close to both the ends of the channel is observed. The temperature at the inlet region gradually increased whereas in the outlet region, temperature falls down to achieve the bulk temperature at the right end. The heat generation is highest at the region filled by low conducting electrolyte (TE) and leads a high temperature plateau.

An inclination of temperature profile arises in the overlapped regions of successive electrolytes. A similar temperature plateau of smaller value observed in the capillary due to presence of electrolytes with high conducting electrolyte (LE). In the region filled by TE (near the inlet region), the electric field strength is higher than that of the region filled by LE region. The outflow of the low conducting TE from inlet reservoir increases with time that leads an increment in axial temperature across the channel which influences the migration speed of the individuals.

Fig. 3 illustrate the normalized concentration profiles across the channel for three electric field strength $E_0(= 7.5 \times 10^3, 10^4 \; and \; 1.25 \times 10^4 V/m)$ at time $t = 120s$. The volumetric heat generation into the system due to Joule heating effect is proportional to the square of the applied electric field and it results a high temperature profile across the channel. Higher temperature values across the channel makes a significant change in electrophoretic migration speed of analytes. High electric field strength speeds up the analytes and the temperature dependence on electrophoretic velocity becomes significant and it justifies the consideration of temperature dependence physical properties.

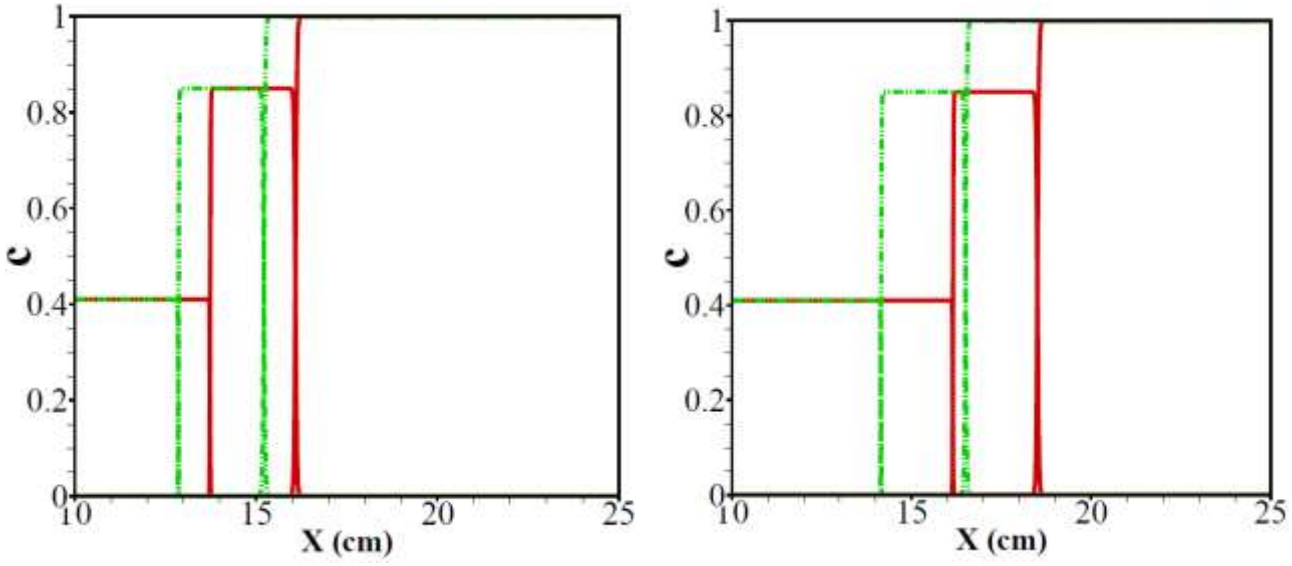

(a) (b)

ISSN 2278-2540 | DOI: 10.51583/IJLTEMAS | Volume XV, Issue VIII, August 2026

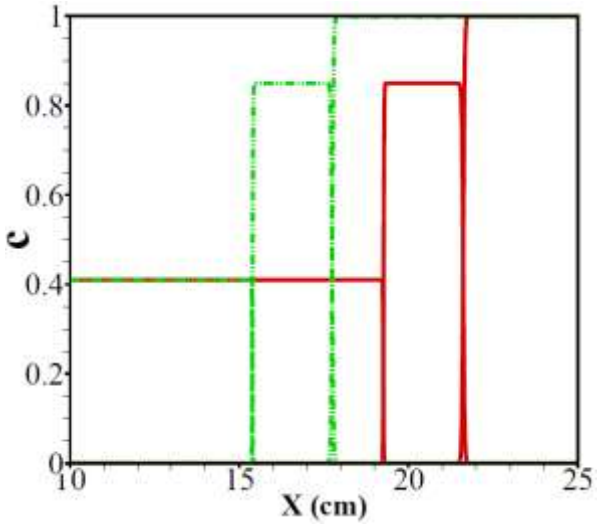

(c)

Figure 3. Concentration distribution of ion across the channel by taking dependent/independent electrical conductivity for electric field strength (a) $E_0 = 7.5 \times 10^3 V/m$; (b) $E_0 = 10^4 V/m$; and $E_0 = 1.25 \times 10^4 V/m$ at time $t = 120s$. The concentration of the LE is taken to be $C_l^{\infty} = 10^{-3} M$ and the mass of the sample species (Sample-1) present in the system $M_s = 20mm \times HC_l^{\infty}$. The solid line represent the case when the electrical conductivity is depend on temperature and dotted line for temperature independent conductivity.

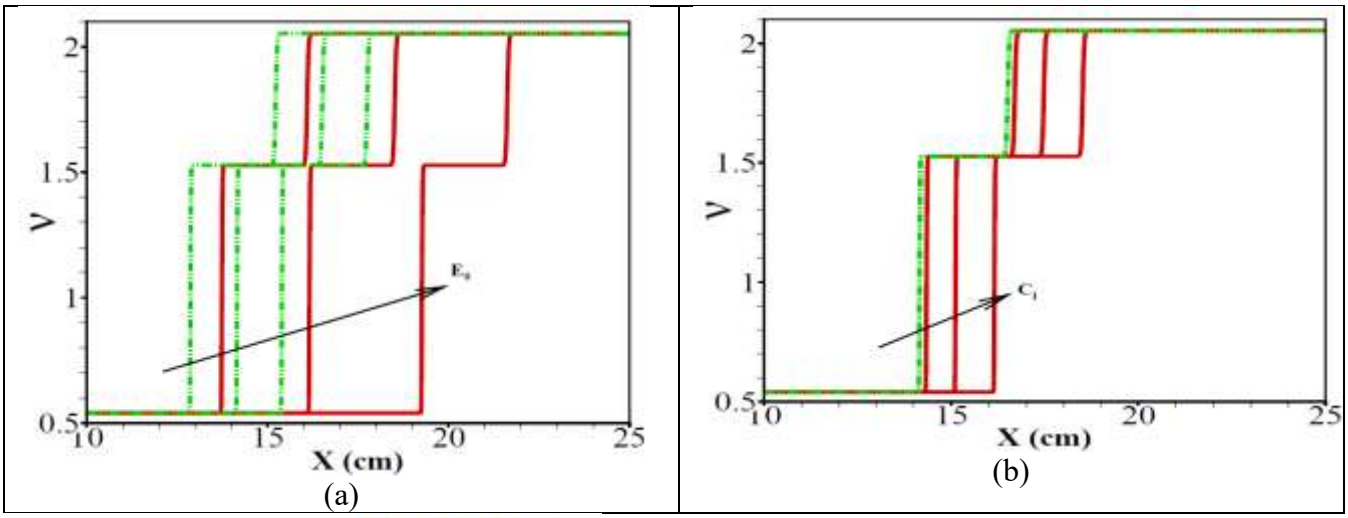

(a) (b)

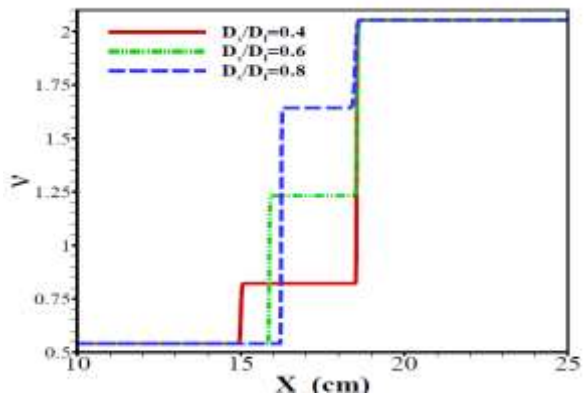

(c)

Figure 4. Conductivity of electrolyte solution across the channel at time $t = 120s$ by taking temperature dependent/independent electrical conductivity by changing (a) electric field strength $E_0 = 7.5 \times 10^3, 10^4 \; and \; 1.25 \times 10^4 V/m$; (b) concentration of the LE $C_l^{\infty} = 10^{-4}, 5 \times 10^{-4}, 10^{-3} M$; (c) diffusivity ration

ISSN 2278-2540 | DOI: 10.51583/IJLTEMAS | Volume XV, Issue VIII, August 2026

of sample species with LD (D_s/D_l). The mass of the sample species (Sample-1) present in the system $M_s = 20mm \times HC_l^{\infty}$. The solid line represent the case when the electrical conductivity is depends on temperature and dotted line for temperature independent conductivity.

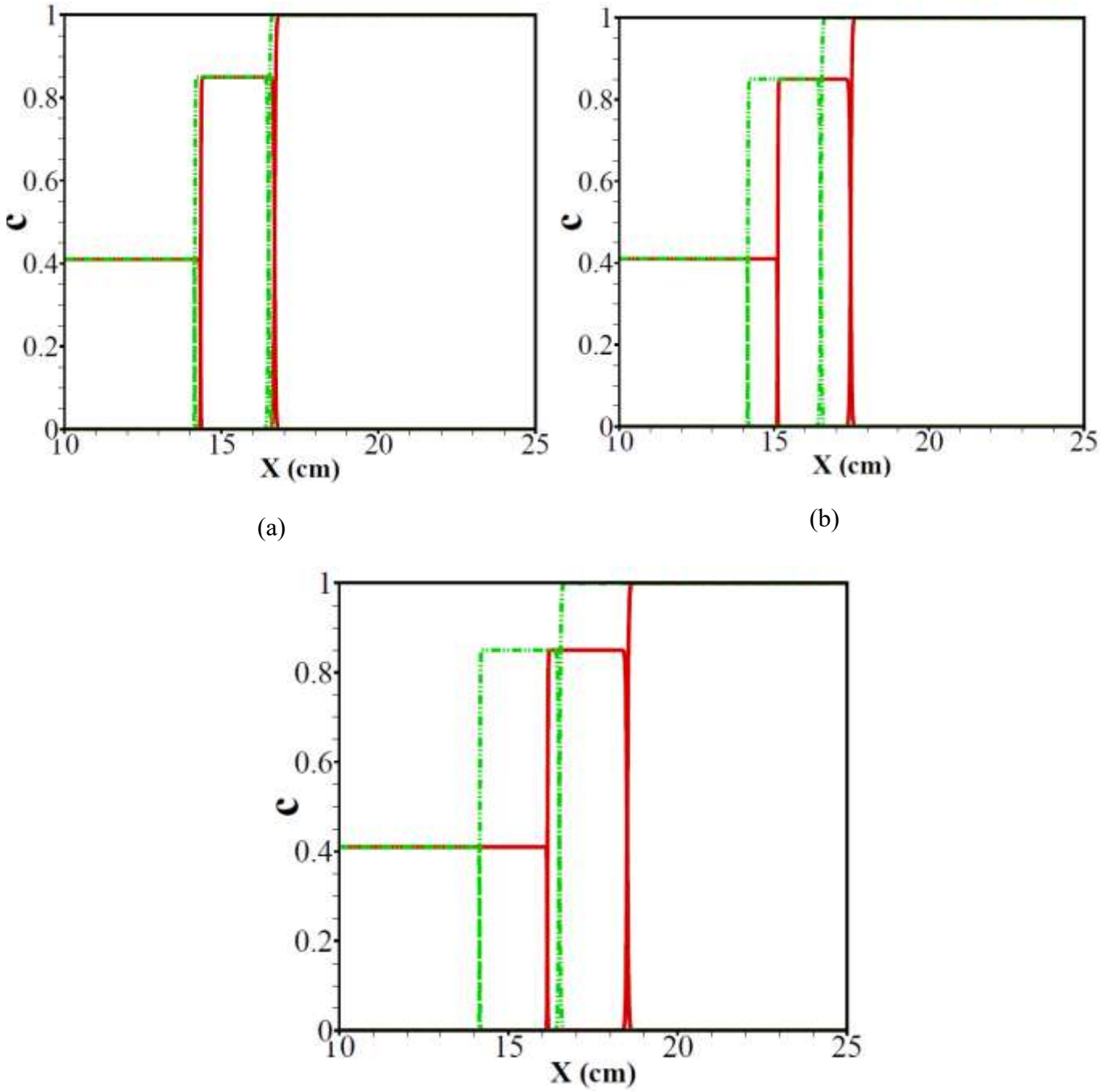

(a) (b)

(c)

Figure 5. Concentration distribution of ions across the channel by taking the temperature dependent/independent electrical conductivity for electric field strength $E_0 = 10^4 V/m$ at time $t = 120s$. The concentration of the LE is taken to be (a) $C_l^{\infty} = 10^{-4}M$; (b) $C_l^{\infty} = 5 \times 10^{-4}M$; (c) $C_l^{\infty} = 10^{-3}M$, and the mass of the sample species (Sample-1) present in the system is $M_s = 20mm \times HC_l^{\infty}$. The solid line represents the case when the electrical conductivity depends on temperature, and the dotted line represents temperature-independent conductivity.

ISSN 2278-2540 | DOI: 10.51583/IJLTEMAS | Volume XV, Issue VIII, August 2026

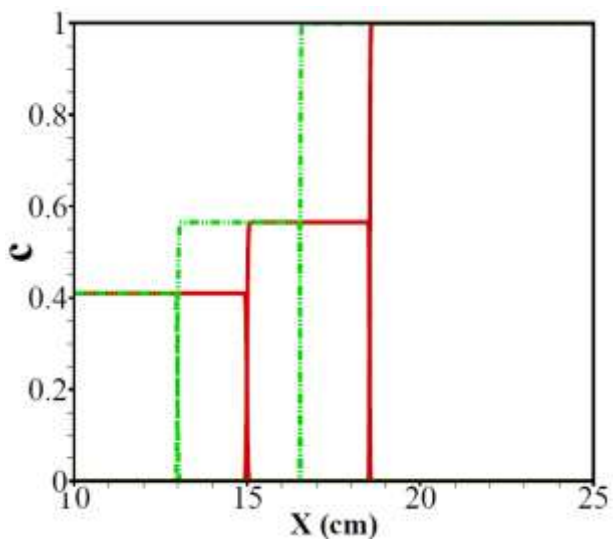

(a)

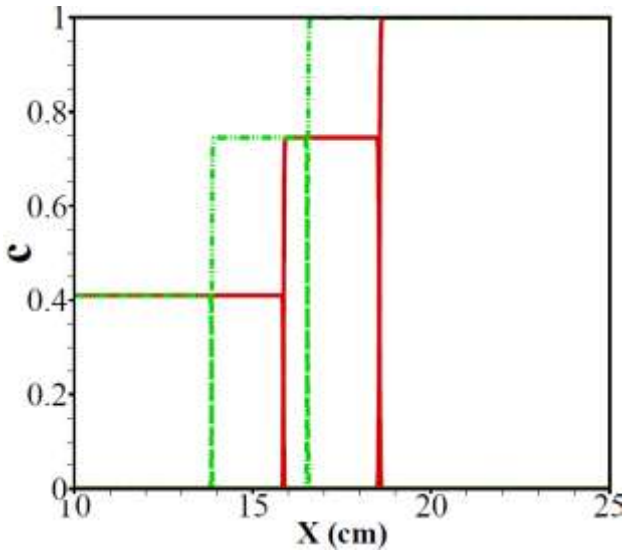

(b)

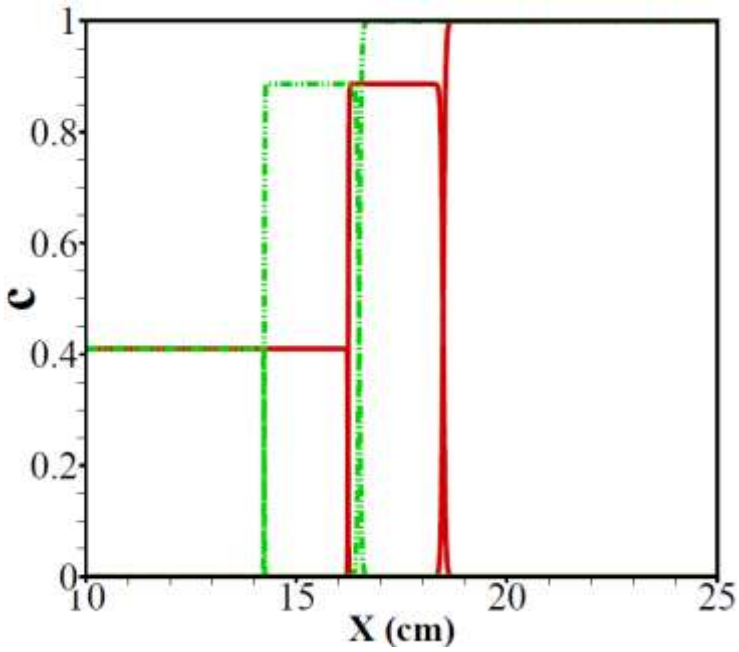

(c)

Figure 6. Concentration distribution of ions across the channel by taking the temperature dependent/independent electrical conductivity for the diffusivity ratio of sample species with LE (D_s/D_l) (a) $(D_s/D_l) = 0.4$; (b) $(D_s/D_l) = 0.4$; and (c) $(D_s/D_l) = 0.8$ at time $t = 120s$. The concentration of the LE is taken $C_l^{\infty} = 10^{-3}M$ and the mass of the sample species present in the system $M_s = 20mm \times HC_l^{\infty}$ with $E_0 = 10^4 V/m$. The solid line represents the case when the electrical conductivity depends on temperature, and the dotted line represents temperature-independent conductivity.

ISSN 2278-2540 | DOI: 10.51583/IJLTEMAS | Volume XV, Issue VIII, August 2026

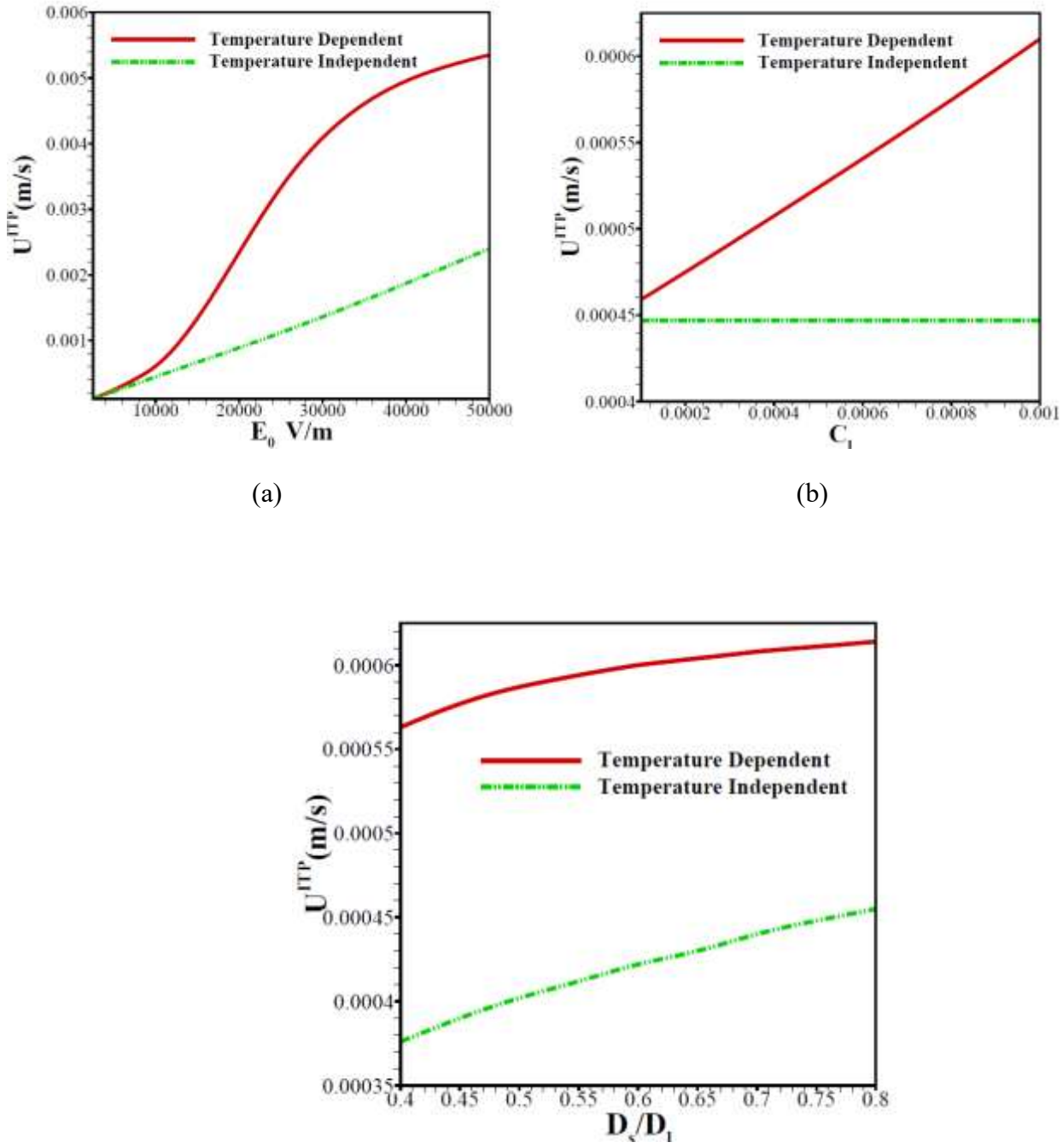

Figure 7. Variation of migration speed of the ionic species by taking the temperature dependent/independent electrical conductivity by changing (a) electric field strength ($E_0 = 7.5 \times 10^3, 10^4\ and\ 1.25 \times 10^4 V/m$); (b) concentration of the LE $C_l^{\infty} = 10^{-4}M, 5 \times 10^{-4}, 10^{-3}M$; (c) diffusivity ratio of sample species with LE (D_s/D_l). The mass of the sample species (Sample-1) present in the system $M_s = 20mm \times HC_l^{\infty}$. The solid line represent the case when the electrical conductivity is depends on temperature and dotted line for temperature conductivity.

Fig. 4 illustrate the normalized conductivity of the electrolyte by changing electric field strength ($E_0 = 7.5 \times 10^3, 10^4\ and\ 1.25 \times 10^4 V/m$); concentration of the LE $C_l^{\infty} = 10^{-4},\ 5 \times 10^{-4},\ 10^{-3}M$; and diffusivity sample species with LE (D_s/D_l). We found that the Joule heating induced temperature greatly effect the overall electrolyte conductivity. When the diffusivity of the sample species is close to TE (i.e., $D_s = 0.4D_l$, the spreading of the sample electrolyte is higher across the channel and the dispersion is gradually decreases if we choose the diffusivity of sample electrolyte close to that of the LE. A steep change in conductivity of the electrolyte across the channel occur since the channel is filled by non-uniform buffer.

ISSN 2278-2540 | DOI: 10.51583/IJLTEMAS | Volume XV, Issue VIII, August 2026

Fig. 5 presents the concentration profiles tor three different solution concentration $C_l^{\infty} = 10^{-4}$, 5×10^{-4}, $10^{-3}M$ with fixed electric field strength $E_0 = 10^4 V/m$. The mass of the sample species (Sample-1) present in the system is taken to be $M_s = 20mm \times HC_l^{\infty}$. The volumetric heat generation into the system due to Joule heating effect is a linear function of C_l^{∞}.

Hence, as expected, rising in solution concentration can increase the Joule heating effect.

Fig. 5(a) shows the that the increase in temperature across the channel can safely be neglected for dilute solution. However for high electrolyte concentration, the Joule heating effect under the parameters studies here can produce temperature increment about 65^0C near the TE region (inlet) and an increment 25^0C near the LE region (outlet). This temperature has an impact on the electrophoretic velocity of each individual present in the system. So for strong electrolyte concentration the electrophoretic velocity ionic species are higher. It causes an earlier separation of sample species and formation of steady state stacking of the electrolyte. In Fig. 6 we present the concentration profile by changing the diffusivity of the sample species keeping same LE and TE and we found that the effect of temperature is significant for all the undertaken cases.

Fig. 7(a) presents the variation of ITP-train velocity with electric field strength E_0 for temperature dependent as well as independent cases. It has been well documented that under isothermal condition, the migration speed of ionic species varies linearly with the electric field strength. Where as this relationship ceases to be linear by considering the Joule heating effect. At the higher values of the electric field, separation process occurs rapidly. In addition, the conduction current produces the Joule heating effect, which is also prominent at high electric field strength. So for the separation process it is advantageous but for large E0, rapid increase in internal energy creates an overheat in the device. To get the optimal functionality, one has to take care of such effects to design the fluidic devices. To give a quantative measurement, we present in Fig. 7(b), the variation of ITP velocity of ions by varying the solution concentration. For isothermal case the ITP migration speed of the ions are independent of the solution concentration for constant voltage drop where as for non-isothermal condition (Fig. 7(b)), it is clear that the migration speed greatly influenced by ionic concentration. Temperature induced ITP migration speed of the ionic species linearly varies with the ionic species linearly varies with the ionic concentration. This linear dependence occur since the volumetric heat generation depends linearly with the concentration of the ionic solution. For isothermal case, that the migration speed ITP-train increase when D_s/D_l approaches to 1. By taking the Joule heating effect into account, a similar pattern observed from Fig. 7(c).

CONCLUSION

A numerical study has been employed to investigate the Joule heating effect on isotachophoretic transport of ionic species in straight 2-D microchannel. We found our numerical method based on finite volume by using QUICK scheme can efficiently capture the ITP-process with or with out Joule heating effect. A non-uniform temperature profile since the channel is filled by the electrolyte with different electrophoretic mobility. A high temperature plateau is observed in the inlet region whereas as low temperature plateau occur in the outlet region. We found that temperature across the channel increases gradually with time. The influence of several parameters governing the Joule heating ITP process, like concentration of buffer solution, electric field strength and electrophoretic mobility of the ionic species, are investigated extensively. The inclusion of temperature dependent physical properties can enhance the ITP separation process but rapid increase in internal energy creates an overheat in the device. This study is important for the microfludics designers those who might want to either avoid or exploit the Joule heating effect to get the optimum functionality of the microfludics devices.

REFERENCES

1. L. Chen, J. E. Prest, P. R. Fielden, N. J. Goddard, A. Manz, P. J. R. Day, Miniaturised isotachophoresis analysis, Lab On a Chip, 6, 474-487(2006).
2. Z. Mal´a, P. Gebauer, and P. Bo˘cek. Recent progress in analytical isotachophoresis, Electrophoresis 34, 19- 28(2013).
3. V. Hruska, M. Jaros, B. Gas, Simul 5 Free dynamic simulator of electrophoresis, Electrophoresis 27, 984-991(2006).

ISSN 2278-2540 | DOI: 10.51583/IJLTEMAS | Volume XV, Issue VIII, August 2026

4. W. Thormann, M. C. Breadmore, J. Caslavska, R. A. Mosher, Dynamic computer simulations of electrophoresis: A versatile research and teaching tool, Electrophoresis, 31, 726754(2010).
5. J. W. Yu, Y. Chou, R. J. Yang, High-resolution modeling of isotachophoresis and zone electrophoresis, Electrophoresis, 29, 1048-1057(2008).
6. Y. Chou, R. J. Yang, Numerical solutions for isoelectric focusing and isotachophoresis problems, Journal of Chromatography A, 1217, 394-404(2010).
7. M. Bercovici, S.K. Lelea, J. G. Santiago, Open source simulation tool for elec- trophoretic stacking, focusing, and separation, Journal of Chromatography A, 1216, 1008- 1018 (2009).
8. J. Shim, M. Cho, P. Dutta, "A method to determine quasisteady state in constant voltage mode isotachophoresis", Electrophoresis 32, 988-995(2011).
9. J. Shim, P. Dutta and C. F. Ivory, "Finite-volume methods for Isotachophoretic seperation in microchannels", Numerical Heat Transfer, Part A: Applications, 52, 441- 461(2007).
10. X. Xuan and D. Li, Joule heating effects on peak broadening in capillary zone electrophoresis. J. Micromech. Microeng. 2004, 14, 1171-1180.
11. B. Kates and C. L. Ren, Study of Joule heating effects on temperature gradient in diverging microchannels for isoelectric focusing applications, Electrophoresis 2006, 27, 1967-1976.
12. E. Grushka, R.M. McCormick, J.J. Kirkland, Effect of temperature gradients on the efficiency of capillary zone electrophoresis separations, Anal. Chem. 61(1989) 241.
13. Y. Kang, C. Yang, and X. Huang, Joule Heating Induced Transient Temperature Field and Its Effects on Electroosmosis in a Microcapillary Packed with Microspheres, Langmuir 2005, 21, 7598-7607.
14. A. Rogacs and J. G. Santiago, Temperature Effects on Electrophoresis, Analytical Chemistry, 2013, 85, 5103-5113.
15. J. H. Knox, Thermal effects and band spreading in capillary electro-separation. Chromatographia 1988, 26, 329-337.
16. F. Sch¨onfeld, G. Goet, T. Baier,and S. Hardt, Transition zone dynamics in combined isotachophoretic and electroosmotic transport, Physics of Fluids 21, 092002(2009).
17. T. Baier, F. Sch¨onfeld and S. Hardt, Analytical approximations to the flow field induced by electroosmosis during isotachophoretic transport through a channel, J. Fluid Mech. 682, 101-119(2011).
18. G. Garcia-Schwarz, M. Bercovici, L. A. Marshall and J. G. Santiago, Sample dispersion in isotachophoresis, J. Fluid Mech. 679, 455-475(2011).
19. S. Bhattacharyya and Partha P. Gopmandal, "Numerical study on separation of analytes through isotachophoresis". Communications in Computer and Information Science, 305, 282-292(2012).
20. S. Bhattacharyya, Partha P. Gopmandal, T. Baier and S. Hardt "Sample dispersion in isotachophoresis with Poiseuille counterflow" Physics of Fluids, 25(2013), 022001-15.
21. J. Shim, and P. Dutta, Joule Heating Effect in Constant Voltage Mode Isotachophoresis in a Microchannel, Int. J. Nonlinear Sci. Numer. Simul. 2012; 13(5): 333344.
22. X. Xuan, D. Sinton, D. Li, Thermal end effects on electroosmotic flow in a capillary, International Journal of Heat and Mass Transfer 47 (2004) 31453157.
23. G. Tang, and C. Yang, Numerical modeling of Joule heating induced temperature gradient focusing in microfluidic channels, Electrophoresis, 29 (2008) 10061012.
24. C. A. J. Fletcher, Computation Technique for Fluid Dynamics. vol 2. (1998) Springer, Berlin.
25. B. P. Leonard, "A stable and accurate convective modelling procedure based on quadratic upstream interpolation", Comput. Meth. Appl. Mech. Eng, 19 (1979)(59-98).
26. G. Goet, T. Baier, S. Hardt, "Transport and separation of micron sized particles at isotachophoretic transition zones", Biomicrofluidics 5, 014109(2011).